Morphological transformation during cross-linking of a highly sulfonated poly(phenylene sulfide nitrile) random copolymer

Lee, So Young; Kang, Na Rae; Shin, Dong Won; Lee, Chang Hyun; Lee, Kwan-Soo; Guiver, Michael D.; Li, Nanwen; Lee, Young Moo

Publisher's version / Version de l'éditeur:
https://doi.org/10.1039/c2ee21992a
Energy and Environmental Science, 5, 12, pp. 9795-9802, 2012-10-18

Journal Name

Dynamic Article Links ►

Cite this: DOI: 10.1039/c0xx00000x

www.rsc.org/xxxxxx

PAPER

Morphological Transformation During Cross-linking of Highly Sulfonated Poly(phenylene sulfide nitrile) Random Copolymer

So Young Lee,[a] Na Rae Kang,[b] Dong Won Shin,[a] Chang Hyun Lee,[d] Kwan-Soo Lee,[e] Michael D. Guiver,[b,c] and Young Moo Lee*[a,b]

Received (in XXX, XXX) Xth XXXXXXXXX 20XX, Accepted Xth XXXXXXXXX 20XX

DOI: 10.1039/b000000x

Here we present a new approach of morphological transformation for effective proton transport within ionomers even at partially hydrated states. Highly sulfonated poly(phenylene sulfide nitrile) (XESPSN) random network copolymers were synthesized as alternatives to state-of-the-art perfluorinated polymers such as Nafion®. Cross-linking reaction was effectively conducted at 250 °C by simple thermal trimerisation of ethynyl groups at the chain termini that would morphologically transform the nanophase separation between the hydrophilic and hydrophobic domains, and thus form well-connected hydrophilic nanochannels for dramatically enhanced proton conduction even at partially hydrated conditions. For instance, the proton conductivity of XEPSN60 was 160% higher than that of Nafion® 212 at 80 °C and 50% relative humidity condition. The water uptake and dimensional swelling were also reduced and mechanical properties and oxidative stability were improved after a three-dimensional network formation. These properties of the XESPSN membranes suggest that they are able to be utilized as desirable polymer electrolyte materials in fuel cell applications under partially hydrated environments.

Introduction

Polymer electrolyte fuel cells (PEFCs) are perceived as environmentally friendly energy conversion devices for both transportation and stationary power systems.[1] The polymer electrolyte membrane (PEM), which is a key component determining PEFC performance, should satisfy tough criteria such as low production cost and physico-chemical durability.[2, 3] Another important PEM requirement is fast proton conduction, even under either low relative humidity (RH) or elevated temperature (e.g., the US Department of Energy (DOE) target is > 0.1 $S \cdot cm^{-1}$ at 80 °C and 50% RH)[4], enabling a simplified PEFC water management system design to reduce parasitic power losses.

To date, PEM materials with diverse chemical architectures and additives have been investigated as alternatives to perfluorinated sulfonic acid state-of-the-art ionomers such as Nafion®. The potential candidates are mainly derived from relatively cheap aromatic hydrocarbons, and are composed of hydrophilic and hydrophobic moieties for proton transport and mechanical integrity, respectively. Effective well-connected water structures formation for rapid proton conduction has been achieved by polymer architecture such as multiblock copolymers[5-8], comb-shaped or triblock copolymers[9-12], and highly sulfonatable copolymers[13, 14], side-chain sulfonated polymers[15] etc. However, the proton conductivity is still low under partially hydrated conditions.[16]

A promising strategy to overcome the barrier is to use highly sulfonated copolymers as proton conduction media and, simultaneously, to suppress excessive water-swelling through crosslinking[17], fabrication of organic-inorganic composites[18-20], reinforcement structure formation[21, 22], or hydrophobic post-treatment.[23, 24]

In the present study, self-crosslinkable disulfonated poly(phenylene sulfide nitrile) random copolymer (ESPSN) precursors were prepared via 1) polycondensation and subsequent nucleophilic substitution for the synthesis of starting random copolymers (SPSN) and 2) the incorporation of thermally curable ethynyl units at their termini, respectively. SPSN has a copolymer backbone derived from poly(phenylene sulfide nitrile), a high performance thermoplastic with high thermal stability and mechanical strength.[25-30] The sulfide (–S–) bridge groups can be spontaneously converted into sulfone ($-SO_2-$) groups, when SPSN was exposed to H_2O_2, which is a by-product evolved at the cathode during PEFC operation and forms free radicals associated with membrane degradation. It is well-known that sulfone functionality is more stable than others to radical attack.[31] Thus, the chemical transformation enables SPSN to have improved oxidative stability and extended PEM lifetime.[32] Nitrile (–C≡N) groups form strong dipolar inter-chain interactions with themselves and with sulfonic acid groups, which are believed to contribute to enhanced dimensional stability even under a hydrated state[33] as well as providing a more stable interface formation with Nafion® ionomer in the electrodes.[34] Thermal curing of the terminal ethynyl groups of flexible ESPSN copolymers could maintain relatively high proton conduction capability by minimizing the reduction in chain mobility after the formation of a three-dimensional (3-D) network.

Experimental section

Materials

4,4'-Dichlorodiphenyl sulfone (DCDPS), 4,4'-thiobisbenzene thiol (TBBT), 3-ethylphenol, dimethylacetamide (DMAc) and toluene were purchased from Sigma Aldrich Co. (WI, USA). 2,6-Dichlorobenzonitrile (DCBN), decafluorobiphenyl (DFBP) and potassium carbonate (K_2CO_3) were purchased from TCI Co. (Tokyo, Japan). TBBT and DCBN were purified by recrystallization in dichloromethane and ethanol respectively before use. DCDPS was converted to 3,3'-disulfonate-4,4'-dichlorodiphenyl sulfone (SDCDPS) by using fuming sulfuric acid (40% SO_3, Sigma Aldrich, WI, USA), followed by neutralization with NaOH. SDCDPS and K_2CO_3 were used after vacuum drying at 120 °C for 1 day.

ESPSN Synthesis

ESPSN copolymers were synthesized through sequential polycondensation and nucleophilic substitution. ESPSN60 is given as a representative example. TBBT (2.5041 g, 10 mmol), SDCDPS (3.0294 g, 6.1 mmol), DCBN (0.5676 g, 3.3 mmol), K_2CO_3 (2.0731 g, 15 mmol), DMAc (40 mL) and Toluene (20 mL) were added into a 250 mL four-neck flask equipped with a mechanical stirrer, a Dean-Stark trap, a thermometer and a reflux condenser. After dehydration at 140 °C for 4 h and toluene removal, the solution mixture was heated up to 165 °C. The temperature was maintained at 165 °C for one day. Then, DFBP (0.4198 g, 0.3 mmol) solution in DMAc (10 mL) was added and stirred at 100 °C for 12 h. For incorporating ethynyl groups, 3-ethynylphenol (0.1380 g, 0.3 mmol) in the mixture of DMAc (10 mL) and toluene (10 mL) was added to DFBP-end-capped SPSN solution. After the reaction for 4 h, the resulting viscous polymer solution was precipitated into a mixture of isopropanol/water (70:30 by volumetric percentage). The residual salts were completely removed after hot water treatment repeatedly. ESPSN60 was dried under vacuum at 120 °C for 1 day. A series of ESPSN was prepared by controlling the ratio of SDCDPS to DCBN, using the same synthetic protocols.

Membrane fabrication and thermal curing

Prior to solution casting, each ESPSN solution in DMAc (15 wt.%) was filtered with 0.45 μm PTFE syringe filter and degassed under vacuum. The ESPSN solution cast on clean glass plate was dried at 45 °C for 1 day, 60 °C for 2 h and 120 °C for 1 day for the membrane formation. For thermally cured XESPSN preparation, additional thermal treatment was performed in an oven at 250 °C for 1.4 h. The resulting potassium salt form XESPSN membranes were acidified by treating in 1 M boiling H_2SO_4 solution for 4 h and boiling water for another 4 h. The thickness of the membrane was ~ 60 μm.

Characterization

The structural analysis of cross-linkable ESPSN was performed using ^{1}H NMR spectra (VNMRS600, Bruker, Germany) with d_6-dimethylsulfoxide (d_6-DMSO) as a solvent. The molecular weights of ESPSN were determined by gel permeation chromatography (GPC) with two Styragel® column and a Waters2414 refractive index detector with N-methyl-2-pyrrolidone (NMP) containing 0.05 M LiBr as eluent. Molecular weight was calibrated with a polymethylmethacrylate standard.

Differential scanning calorimetry (DSC, Q20, TA Instruments, USA) was used for determining the degree of cross-linking of ESPSN. Heat flow was observed by isothermal curing at 250 °C for the cross-linking reaction. The preheating rate is 10 °C /min. The degree of cross-linking was calculated as $y = (H_t/H_T) \times 100$, where H_t is the total heat flow of sample mass for a given cross-linking time t and H_T is the total heat flow of sample mass for a cross-linking time for 100 min.

The membrane density was measured after acidification. Before measurement, the membranes were dried in vacuum oven at 120 °C and isooctane (density = 0.693 g/cm^3) was used as the measurement solvent.

For transmission electron microscopy (TEM) observations, the membranes were stained with lead ions by ion exchange of the sulfonic acid groups in 0.5 M lead acetate aqueous solution. To avoid precipitation as well as the oxidation of lead ions, the membranes were stained during short time in the glove box and rinsed several times repeatedly with deionized water, and then dried in a vacuum oven for 12 h. The stained membranes were embedded in epoxy resin, sectioned to 80 nm in thickness with a RMC MTX Ultra microtome, and placed on copper grids. Images were taken with a Carl Zeiss LIBRA 120 energy-filtering transmission electron microscope using an accelerating voltage of 120 kV.

Water uptake (WU) and dimensional change were determined by measuring the weight, area and thickness of acid form membranes before and after hydration. Their initial measurements were made after the membranes were dried under vacuum at 120 °C for 12 h. Then the membranes were immersed in deionized water stirred for one day to reach equilibrium at given temperatures (30 °C and 80 °C). Before weight measurements of the wet membranes, the surface water on the membrane was removed. Weight-based water uptake (WU_w) and volumetric water uptake (WU_v) were calculated with the following equations. Volumetric water uptake (WU_v) was determined from the density of water (δ_w) and the dried membrane (δ_M).

$$\mathrm{WU}_w(\mathrm{wt\%}) = \frac{W_{wet} - W_{dry}}{W_{dry}} \times 100 \quad (1)$$

$$\mathrm{WU}_v(\mathrm{vol\%}) = \frac{(W_{wet} - W_{dry})/\delta_w}{(W_{dry}/\delta_M)} \times 100 \quad (2)$$

Where W_{dry} and W_{wet} are the weights of dried and wet membranes, respectively.

Water swelling of membranes was determined by measuring area (in-plane swelling) and thickness (through-plane swelling) changes in the samples after they were dried at 120 °C for 12 h and soaked in deionized water at both 30 and 80 °C for one day.

$$\text{In}-\text{plane swelling}\ (\%) = \frac{A_{wet} - A_{dry}}{A_{dry}} \times 100 \quad (3)$$

$$\text{Through}-\text{plane swelling}\ (\%) = \frac{l_{wet} - l_{dry}}{l_{dry}} \times 100 \quad (4)$$

Where A_{dry} and A_{wet} are the area of dried and wet membranes, respectively, while l_{dry} and l_{wet} are the thickness of dried and wet membranes, respectively.

The ion exchange capacity (IEC) of membranes was

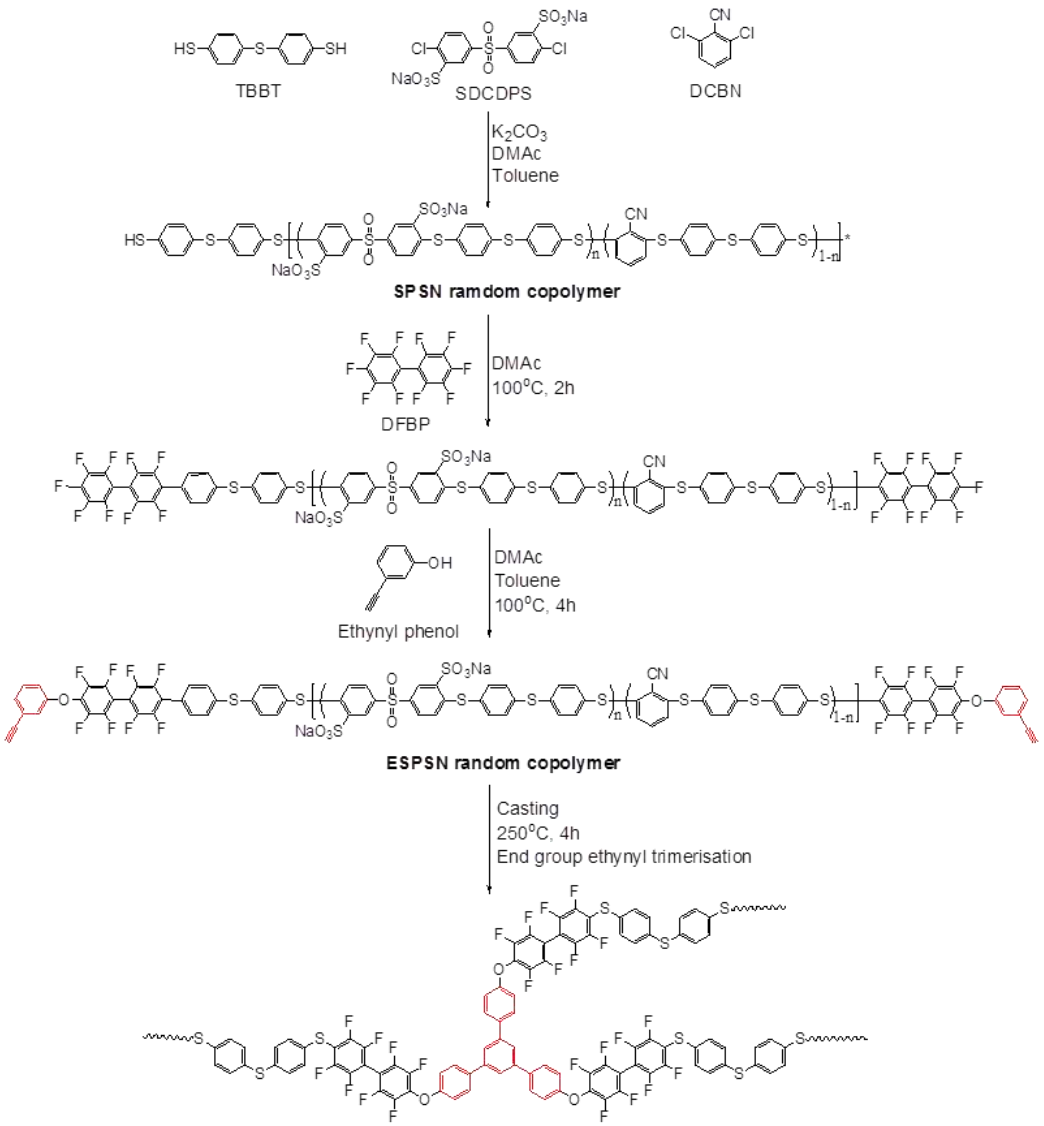

Scheme 1 Synthesis route of the polymer XESPSN

determined by acid-base titration. The acid form membrane samples were soaked in a 1.0 M NaCl solution for one day, and then the solution was titrated with 0.01 M NaOH solution using phenolphthalein as an indicator. The IEC was calculated by the NaOH consumed from the titration and the weight of the dried membrane samples. Volumetric IEC ($IEC_{v(dry)}$) was obtained by multiplying the IEC_w value and the membrane density. The $IEC_{v(wet)}$ was calculated based on water uptake measurements using the following equation.

$$IEC_{v\,(dry)} = IEC_w \times \text{density} \quad (5)$$

$$IEC_{v\,(wet)} = \frac{IEC_v}{1+0.01WU_w\,(vol\%)} \times 100 \quad (6)$$

The tensile strength and elongation of membranes were measured using a universal testing machine (Shimazu, AGS-500NJ, Tokyo, Japan) following ISO37-4. Mechanical properties were measured under dry and wet conditions. Under wet conditions, samples were supplied with continuous humidification.

The proton conductivity of each membrane sample (size : 1 cm × 4 cm) was measured longitudinally under different RH conditions at 80 °C with a four-point probe alternating current (AC) impedance spectrometer (Solartron 1260, Farnborough Hampshire, ONR, UK). The measurements were performed in a thermo- and hydro-controlled chamber in an electronic noise-free environment. The proton conductivity (σ) was calculated from the following equation.

$$\sigma = \frac{L}{RS} \quad (7)$$

Where L is the distance between the counter electrodes and the working electrode, R is the impedance of membrane and S is the cross-sectional surface area of membrane samples (cm^2).

MEA fabrication and single cell performance

Membrane electrode assemblies (MEAs) were fabricated by the catalyst-coated substrate (CCS) method. Nafion perfluorinated

ion-exchange resin solution (DuPont, USA) and 20 wt% Pt/C (Johnson Matthey Fuel Cell, USA) were mixed in water. The catalyst slurry was coated on gas diffusion layers (GDLs), both anode and cathode sides, until the weight of Pt loading reached 0.3 mg/cm^2. MEAs were fabricated by sandwiching the membranes between the anode and cathode electrodes and hot pressed at 130 °C under a pressure of 50 bar for 7 min. The prepared MEAs were tested in a single-cell fixture (with an active area of 5 cm^2). The PEFC tests were performed on single-cell test stations (WonA.Tech, SMART I, Seoul, Korea). Electrochemical performances of cross-linked XESPSN membranes were measured under the following conditions. H_2 and O_2 were supplied at a flow rate of 100 cm^3 at 80 °C under 50% RH.

Results and discussion

The degree of sulfonation (DS) of ESPSN precursors with number average molecular weights (M_n) of 18 to 30 kDa was controlled to 50 to 70 mol%, corresponding to an IEC range of 1.96 to 2.49 meq.g^{-1}. The curing of ESPSN was conducted at 250 °C for 100 min in the solid membrane state via a thermally activated terminal ethynyl group trimerisation mechanism, without catalysts and initiators.[35-39] (Scheme 1)

Cross-linkable ESPSN structures were characterized by ^{1}H NMR. As shown in Fig. 1, ^{1}H NMR spectra showed clear trends with changing DS. The signal intensities at 8.2 ppm (peak 1), 7.7 ppm (peak 2) and 6.9 ppm (peak 3) corresponding to the disulfonated group (SDCDPS) increased with the degree of sulfonation. On the other hand, the signal at 7.2 ppm (peak 6) corresponding to the DCBN moiety of the hydrophobic part decreased. The small signal at 4.2 ppm (peak 7) was assigned to the terminal ethynyl proton. ^{1}H NMR spectra confirmed the cross-linkable ESPSN was synthesized as desired.

To verify the degree of cross-linking with the curing time, heat flow of XESPSN60 was observed by DSC isotherm experiments at 250 °C for up to 100 min (Fig. 2). Exothermic heat flow was observed as the cross-linking reaction proceeded. About 80% of the thermal curing reaction took place within 20 min. After the thermal treatment for about 100 min, cross-linking was terminated.

After the thermal treatment, 3-D network formation was confirmed via solubility tests, and gel-fraction measurements. At 30 °C, XESPSN membranes were insoluble in polar aprotic solvents such as DMAc and N-methylpyrrolidone (NMP), which are good solvents for the precursor ESPSN. The degree of

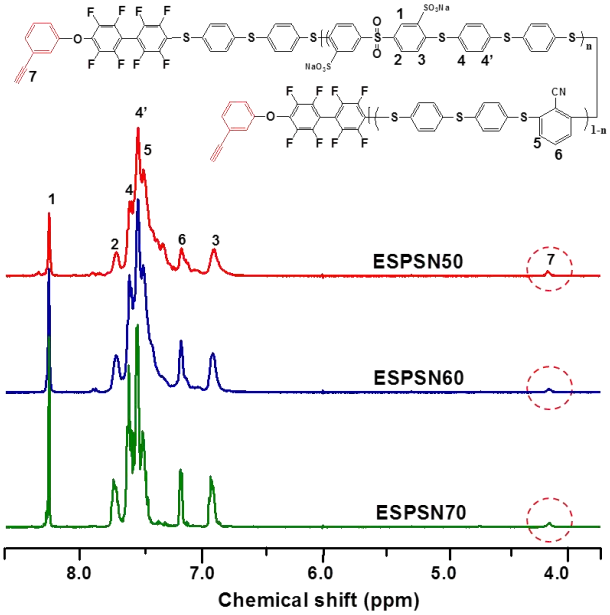

Fig. 1 ^{1}H NMR spectra of ESPSN

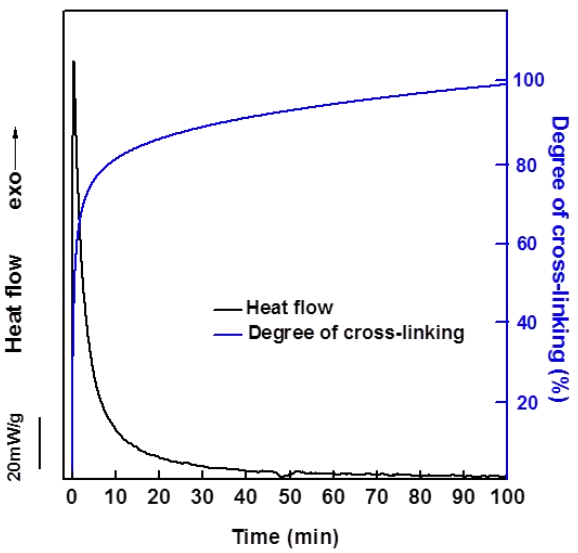

Fig. 2 Degree of cross-linking of ESPSN60 with cross-linking reaction time

Table 1 Molecular weight, mechanical strength and solubility of ESPSN and XESPSN copolymers

Copolymer	DS [mol.%]	Mn[a] [kDa]	PDI[a]	Tensile strength[b] [MPa]		Elongation at break[b] [%]		Young's modulus[b] [MPa]		Solubility in DMAC	Gel fraction[c] [%]
				Dry	Wet	Dry	Wet	Dry	Wet		
ESPSN50	50	17.5	3.22	33.9 ± 8.7	17.1 ± 3.2	21.9 ± 2.3	22.0 ± 4.6	10	82	Yes	-
ESPSN60	60	29.5	2.77	44.5 ± 5.4	29.9 ± 3.9	31.4 ± 1.0	131.7 ± 13.2	21	129	Yes	-
ESPSN70	70	25.6	3.4	30.9 ± 5.4	13.9 ± 5.0	10.1 ± 0.4	103.8 ± 9.7	10	32	Yes	-
XESPSN50	50	-	-	46.9 ± 4.4	20.2 ± 0.4	10.0 ± 0.2	50.1 ± 16.9	11	251	Swollen	97.3
XESPSN60	60	-	-	59.9 ± 4.2	32.5 ± 1.2	15.2 ± 2.1	153.9 ± 15.3	25	380	Swollen	97.1
XESPSN70	70	-	-	69.0 ± 3.1	15.7 ± 1.1	13.7 ± 0.4	102.8 ± 7.40	13	117	Swollen	97.9
Nafion 212	-	-	-	22.5 ± 2.9	19.5 ± 0.3	200.4 ± 12.3	224.6 ± 10.6	2.3	50	-	-

[a] Determined by GPC using NMP with 0.05 M LiBr. [b] Measured at 30 °C. [c] Gel fraction was obtained from the ratio of the weight of polymer after extraction from DMAc at 80 °C for 1 day and the initial weight.

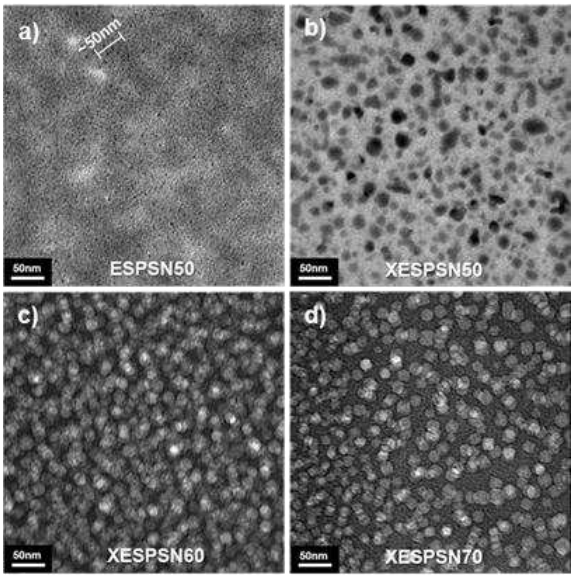

Fig. 3 a) TEM images of ESPSN50 precursor (a), XESPSN50 (b), XESPSN60 (c), and XESPSN70 (d)

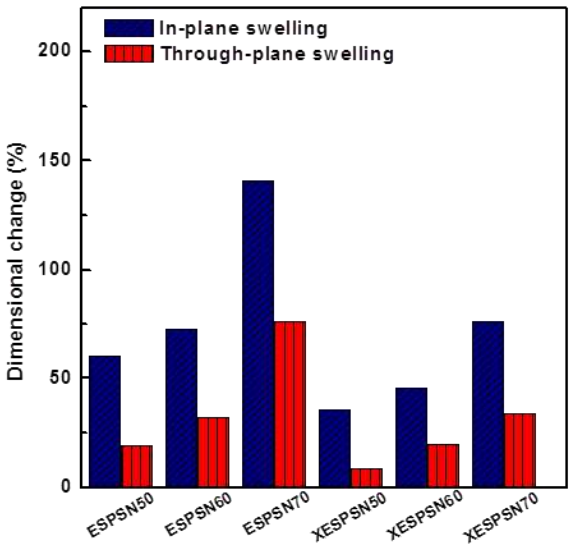

Fig. 4 Dimensional swelling of ESPSN and XESPSN in water at 30 °C

crosslinking, based on the gel fraction, was over 97% (Table 1). Note that the mechanical properties of XESPSN were significantly improved when compared with those of ESPSN in the fully hydrated state. XESPSN exhibited mechanical toughness and stiffness comparable to Nafion® 212. In the dry state, the tensile strength of XESPSN was ~155% higher than those of ESPSN. However, elongation at break of XESPSN was about ~50 % of ESPSSN. Improved tensile strength and reduction of elongation in the dry state of XESPSN is due to the presence of the cross-linking between polymer chains, which increased rigidity and strength of the polymer chains.

The cross-sectional nanophase-morphologies of ESPSN and XESPSN membranes (Fig. 3a-d) were obtained through transmission electron microscopy (TEM). The dark phase represents hydrophilic domains composed of sulfonate groups with lead counter cations. The hydrophilic domains in ESPSN are randomly distributed within the hydrophobic matrix shown as the bright phase (Fig. 3a), with morphological features similar to many random copolymers having high IEC values; the size of the hydrophilic domains appears to be relatively large (> 50 nm) and hydrophilic-hydrophobic phase separation is less developed. Surprisingly, thermally cured XESPSN copolymers exhibited well-defined, nanophase-separated morphologies (Fig. 3b-d), in spite of using random copolymer precursors. Their morphological transformation may be associated with thermally induced molecular rearrangement leading to the self-aggregation of both hydrophilic and hydrophobic moieties. Their morphological characteristics are highly dependent on their DS values. Relatively low DS XESPSN50 exhibits hydrophilic spheroidal clusters with non-uniform diameter size of 10-25 nm within interconnected hydrophobic copolymer phases (Fig. 3b), while XESPSN60 shows a worm-like morphology with bi-continuous hydrophilic and hydrophobic network in narrow diameter ranges of 15-20 nm and 20-25 nm, respectively (Fig. 3c). For higher DS values of 60 to 70 mol. %, the size of the interconnected hydrophilic domains increased up to 40 nm, while hydrophobic domain size was somewhat reduced. Note that the morphological inversion between hydrophilic and hydrophobic phases became distinct as DS values increased. These unusual and unique phase changes are expected to influence the proton transport behaviour through XESPSN networks, particularly in a partially hydrated state.

Appropriate hydration of PEM materials is important in balancing proton conductivity and mechanical strength simultaneously. Linear copolymers with high DS values generally show high proton conductivity, but their excessive water swelling

Table 2 Properties and stability of ESPSN and XESPSN membranes.

Copolymer	Density[a] [g cm^{-3}]	IEC[b] [meq.g^{-1}]	IEC$_{v(dry)}$ [meq.cm^{-3}]	IEC$_{v(wet)}$ [meq.cm^{-3}]	WU[c] [%]	λ[d]	σ[e] [Scm^{-1}]	Oxidative stability[f] [wt.%]	τ[g] [h]
ESPSN50	1.23	1.96	2.41	1.51	47.7	13.5	0.12	104.1	6.3
ESPSN60	1.25	2.20	2.75	1.53	64.1	16.2	0.16	NA[h]	NA[h]
ESPSN70	1.26	2.49	3.13	0.94	182.6	40.7	0.18	NA[h]	NA[h]
XESPSN50	1.23	2.02	2.48	1.81	29.8	8.2	0.15	111.6	7.3
XESPSN60	1.26	2.28	2.87	1.92	38.9	9.4	0.18	105.7	5.5
XESPSN70	1.28	2.53	3.23	1.15	140.5	30.8	0.20	104.3	3.5
Nafion 212	1.97	0.98	1.93	1.28	21.6	12.2	0.11	98.0	> 50

[a] Measured from a known membrane dimension and weight after drying at 120ºC for 1 day. [b] Determined by titration. [c] Water uptake (WU) at 30 ºC. [d] Hydration number = the mole ratios of H_2O to SO_3H [e] Proton conductivity at 30 ºC in water. [f] Residual weight percent of membranes after in Fenton's test. [g] the time when the membranes dissolved completly. [h] Not applicable: membrane formed hydrogel or dissolved

results in mechanical failures, particularly at interfaces with PEFC electrodes.[4] At DS values over their percolation threshold, extremely high water uptake dilutes the concentration of sulfonic acid groups per copolymer volume ($IEC_{v(wet)}$), which often induces proton conductivity much lower than theoretical values.[40, 41] This dilution effect on $IEC_{v(wet)}$ is obviously apparent in ESPSN70 whose DS is higher than the percolation threshold to WU and λ (i.e., ESPSN60) (Table 2). Consequently, the proton conductivity and $IEC_{v(wet)}$ of ESPSN70 is lower than what would be expected in a linearly increasing conductivity trend. After crosslinking, membrane water uptake and water swelling ratios (Fig. 4) were reduced by ~ 48% and 25-38%, respectively, when compared to ESPSN. The water uptake losses led to dramatically improved $IEC_{v(wet)}$ in the fully hydrated state (Table 2). Consequently, XESPSN exhibited proton conductivity superior to the corresponding ESPSN precursors and Nafion® 212, used as a reference. The rapid proton transport through XESPSN in water at 30 °C resulted from a synergetic effect of 3-D network formation-induced morphological transformation into well-defined hydrophilic-hydrophobic nanophase-separated domains and chain flexibility (as demonstrated by high elongation values in Table 1), in addition to its enhanced ionic concentration. The results also imply a high degree of connectivity within the proton-conducting hydrophilic phase.

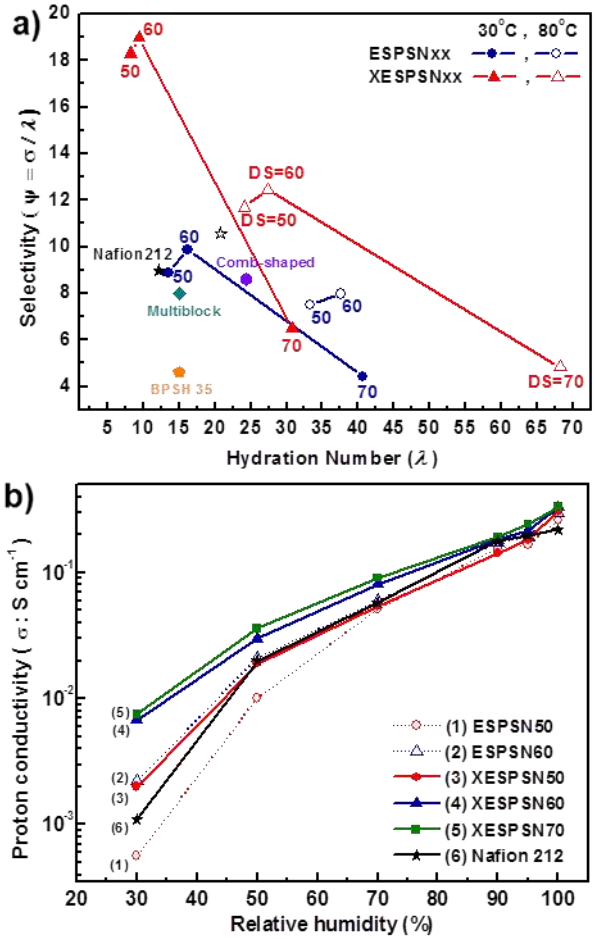

Fig. 5 a) ψ for ESPSN, XESPSN membranes and Nafion®212 at 30°C and 80°C in fully hydration state and b) σ at different RH values and 80 °C.

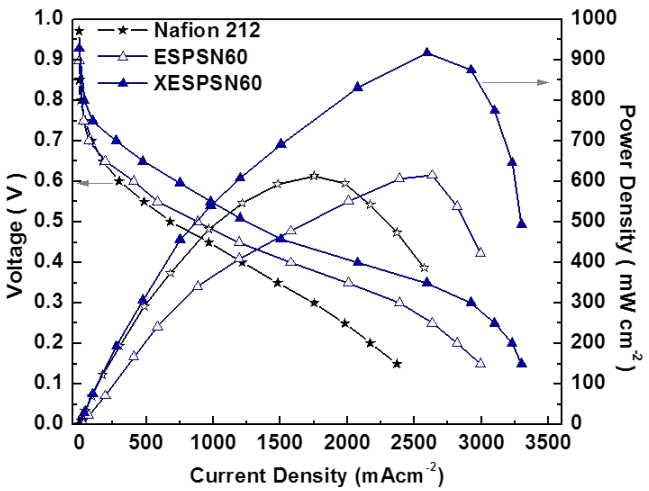

Fig. 6 H_2/O_2 PEFC performance of ESPSN60, XESPSN60 and Nafion® 212 at 80 °C with humidification at 50% RH

Fig. 5a shows selectivity ($\psi = \sigma / \lambda$)[7] as a function of hydration number (λ) at 30 and 80 °C in fully hydration conditions respectively. The ψ values of XESPSN50 and 60 are higher than those of corresponding ESPSN PEMs and Nafion® 212. This implies that water molecules in XESPSN are more effectively utilized for proton transport as compared to other PEMs. For instance, XESPSN60 has ψ values higher than other highly phase-developed PEM materials including multiblock[7] and comb-shaped copolymers[10] at similar hydration levels.

Interestingly, the favourable effect of 3-D network formation through end-group crosslinking on proton conduction was especially evident in partially hydrated states. Proton conductivities decreased with decreasing humidity, irrespective of which PEM materials were used (Fig. 5b). This reduction in proton transport capability with decreasing RH or dry states is typically observed and is associated with evaporation of proton carrier water molecules.[42] However, after 3-D network formation, the extent of proton conductivity reduction was largely alleviated in the measured RH range. Most significantly, the proton conductivity of XESPSN60 under RH 30% was 320% and 680% higher than those of ESPSN60 and Nafion® 212, respectively. The improved proton conduction observed in XESPSN is due to ordered nanophase morphology by high local density of sulfonic acid groups within the hydrophilic domain during cross-linking.

The oxidative stability, which indirectly shows PEM durability to free radical attack, was evaluated by comparing the PEM weight changes after soaking in Fenton's reagent (3 wt.% H_2O_2 containing 2 ppm $FeSO_4$) at 80 °C for 1 h.[43] The time elapsed until complete membrane dissolution (τ) was also measured under the same conditions and is summarized in Table 2. All PEM materials except ESPSN60 and 70 showed modest weight gains as a result of oxidation from –S– to $–SO_2–$. ESPSN60 and 70 dissolved in Fenton's reagent. However, the cross-linked counterparts XESPSN exhibited comparatively more stable oxidative resistance after the end-group curing, and thus were expected to show chemical resistance to PEM degradation under PEFC operation conditions.

Fig. 6 shows the current-voltage polarization curves of XESPSN60, ESPSN60, and Nafion® 112, which were obtained at 80 °C and 50% RH. All single cells were made using the same fabrication procedures and electrode composition in order to isolate the PEM contribution from PEFC performance.[44] XESPSN60 demonstrated the highest PEFC performance among the tested samples. At 0.6 V, its current density and maximum power density were ~160% and ~150% higher than those of ESPSN60 and Nafion® 212, respectively.

Conclusions

In summary, a promising PEM material, XESPSN, was synthesized via polycondensation of SPSN copolymers with high DS values. The incorporated thermally curable ethynyl groups at the termini of the starting copolymers (ESPSN) led to 3-D network formation, resulting in unusual morphological transformation. XESPSN has well-developed hydrophilic-hydrophobic nanophase separation, high sulfonic acid density, and retains chain mobility for maintaining fast proton transport even in partially hydrated states. XESPSN showed outstanding low humidity PEFC performance when compared with other hydrocarbon PEM materials or Nafion® used in PEFCs.

Acknowledgements

This research was supported by the WCU (World Class University) program through the National Research Foundation of the Korean Ministry of Science and Technology (No. R31-2008-000-10092-0) and New & Renewable Energy R&D program (2008-N-FC12-J-01-2-100) under the Ministry of Knowledge Economy.

Notes references

[a] *School of Chemical Engineering, College of Engineering Hanyang University, Seoul 133-791, Republic of Korea. E-mail: ymlee@hanyang.ac.kr*
[b] *WCU Department of Energy Engineering, Hanyang University, Seoul 133-791, Republic of Korea.*
[c] *Institute for Chemical Process and Environmental Technology, National Research Council, Ottawa, Ont, KIA OR6, Canada*
[d] *Department of Green Energy Engineering, College of Engineering, Uiduk University, Gyeongju 780-713, Republic of Korea*
[e] *The 6th Research Team, Daedeok Research Institute, Honam Petrochemical Corp., Daejeon 305-726, Republic of Korea*
These authors contributed equally to this work.

1. C. E. Heath and A. G. Revfsz, *Science*, 1973, **180**, 542-544.
2. M. A. Hickner, H. Ghassemi, Y. S. Kim, B. R. Einsla and J. E. McGrath, *Chem. Rev.*, 2004, **104**, 4587-4612.
3. M. Rikukawa and K. Sanui, *Prog. Polym. Sci.*, 2000, **25**, 1463-1502.
4. C. H. Park, C. H. Lee, M. D. Guiver and Y. M. Lee, *Prog. Polym. Sci.*, 2011, **36**, 1443-1498.
5. K. B. Wiles, C. M. de Diego, J. de Abajo and J. E. McGrath, *J. Membr. Sci.*, 2007, **294**, 22-29.
6. H.-S. Lee, A. Roy, O. Lane, S. Dunn and J. E. McGrath, *Polymer*, 2008, **49**, 715-723.
7. A. Roy, X. Yu, S. Dunn and J. E. McGrath, *J. Membr. Sci.*, 2009, **327**, 118-124.
8. B. Bae, T. Yoda, K. Miyatake, H. Uchida and M. Watanabe, *Angew. Chem. Int. Ed.*, 2010, **49**, 317-320.
9. D. S. Kim, G. P. Robertson and M. D. Guiver, *Macromolecules*, 2008, **41**, 2126-2134.
10. N. Li, C. Wang, S. Y. Lee, C. H. Park, Y. M. Lee and M. D. Guiver, *Angew Chem Int Edit*, 2011, **50**, 9158-9161.
11. N. Li, S. Y. Lee, Y.-L. Liu, Y. M. Lee and M. D. Guiver, *Energy Environ. Sci.*, 2012, **5**, 5346-5355.
12. G. Dorenbos and K. Morohoshi, *Energy Environ. Sci.*, 2010, **3**, 1326-1338.
13. S. Matsumura, A. R. Hlil, C. Lepiller, J. Gaudet, D. Guay, Z. Shi, S. Holdcroft and A. S. Hay, *Macromolecules*, 2007, **41**, 281-284.
14. S. Matsumura, A. R. Hlil, N. Du, C. Lepiller, J. Gaudet, D. Guay, Z. Shi, S. Holdcroft and A. S. Hay, *J. Polym. Sci., Part A: Polym. Chem.*, 2008, **46**, 3860-3868.
15. C. Wang, N. Li, D. W. Shin, S. Y. Lee, N. R. Kang, Y. M. Lee and M. D. Guiver, *Macromolecules*, 2011, **44**, 7296-7306.
16. R. Devanathan, *Energy Environ. Sci.*, 2008, **1**, 101-119.
17. J. A. Kerres, *Fuel Cells*, 2005, **5**, 230-247.
18. A. M. Herring, *Journal of Macromolecular Science, Part C: Polymer Reviews*, 2006, **46**, 245-296.
19. K. Miyatake, T. Tombe, Y. Chikashige, H. Uchida and M. Watanabe, *Angew. Chem. Int. Ed.*, 2007, **46**, 6646-6649.
20. G. L. Athens, Y. Ein-Eli and B. F. Chmelka, *Adv. Mater.*, 2007, **19**, 2580-2587.
21. T. Yamaguchi, H. Zhou, S. Nakazawa and N. Hara, *Adv. Mater.*, 2007, **19**, 592-596.
22. J. B. Ballengee and P. N. Pintauro, *Macromolecules*, 2011, **44**, 7307-7314.
23. C. H. Lee, S. Y. Lee, Y. M. Lee, S. Y. Lee, J. W. Rhim, O. Lane and J. E. McGrath, *ACS Appl. Mater. Interfaces*, 2009, **1**, 1113-1121.
24. S. J. Lue, S.-Y. Hsiaw and T.-C. Wei, *J. Membr. Sci.*, 2007, **305**, 226-237.
25. Z. Bai, M. F. Durstock and T. D. Dang, *J. Membr. Sci.*, 2006, **281**, 508-516.
26. K. B. Wiles, F. Wang and J. E. McGrath, *J. Polym. Sci., Part A: Polym. Chem.*, 2005, **43**, 2964-2976.
27. Z. Bai, M. D. Houtz, P. A. Mirau and T. D. Dang, *Polymer*, 2007, **48**, 6598-6604.
28. H. Dai, H. M. Zhang, Q. T. Luo, Y. Zhang and C. Bi, *J. Power Sources*, 2008, **185**, 19-25.
29. J. K. Lee and J. Kerres, *J. Membr. Sci.*, 2007, **294**, 75-83.
30. M. Schuster, C. C. de Araujo, V. Atanasov, H. T. Andersen, K.-D. Kreuer and J. Maier, *Macromolecules*, 2009, **42**, 3129-3137.
31. M. Schuster, K.-D. Kreuer, H. T. Andersen and J. Maier, *Macromolecules*, 2007, **40**, 598-607.
32. D. S. Phu, C. H. Lee, C. H. Park, S. Y. Lee and Y. M. Lee, *Macromol. Rapid Commun.*, 2009, **30**, 64-68.
33. Y. S. Kim, D. S. Kim, B. Liu, M. D. Guiver and B. S. Pivovar, *J. Electrochem. Soc.*, 2008, **155**, B21-B26.
34. D. S. Kim, Y. S. Kim, M. D. Guiver and B. S. Pivovar, *J. Membr. Sci.*, 2008, **321**, 199-208.
35. K.-S. Lee and J.-S. Lee, *Chem. Mater.*, 2006, **18**, 4519-4525.
36. J.-P. Kim, W.-Y. Lee, J.-W. Kang, S.-K. Kwon, J.-J. Kim and J.-S. Lee, *Macromolecules*, 2001, **34**, 7817-7821.
37. M.-H. Jeong, K.-S. Lee and J.-S. Lee, *J. Membr. Sci.*, 2009, **337**, 145-152.
38. K.-S. Lee, M.-H. Jeong, J.-P. Lee and J.-S. Lee, *Macromolecules*, 2009, **42**, 584-590.
39. M.-H. Jeong, K.-S. Lee and J.-S. Lee, *Macromolecules*, 2009, **42**, 1652-1658.
40. Y. S. Kim and B. S. Pivovar, *Annu. Rev. Chem. Biomol. Eng.*, 2010, **1**, 123-148.
41. C. H. Lee, K.-S. Lee, O. Lane, J. E. McGrath, Y. Chen, S. Wi, S. Y. Lee and Y. M. Lee, *RSC Advances*, 2012, **2**, 1025-1032.
42. K.-D. Kreuer, *Chem. Mater.*, 1996, **8**, 610-641.
43. N. Asano, M. Aoki, S. Suzuki, K. Miyatake, H. Uchida and M. Watanabe, *J. Am. Chem. Soc.*, 2006, **128**, 1762-1769.
44. D. S. Hwang, C. H. Park, S. C. Yi and Y. M. Lee, *Int. J. Hydrogen Energy*, 2011, **36**, 9876-9885.